HAYATI
Journal of Biosciences

Vol. 30 No. 3, May 2023 480-490
DOI:10.4308/hjb.30.3.480-490
ISSN: 1978-3019
EISSN: 2086-4094

In Silico Analysis of 14-Deoxy 11, 12-Didehydro Andrographolide (AGP 2) From Sambiloto (*Andrographis paniculata*) As Drug Candidate Against SARS-CoV-2

Muhammad Vicky Astria[1], Lud Waluyo[1*], Roimil Latifa[1], Moh. Mirza Nuryady[1], Rr. Eko Susetyarini[1], Mohd. Affendi bin Labo[2]

[1]*Department of Biology Education, Faculty of Teacher Training and Education, University of Muhammadiyah Malang, Malang 65144, Indonesia*
[2]*Department of Chemical Engineering, School of Chemical Engineering, University of Technology MARA, 40451 Shah Alam, Selangor, Malaysia*

ARTICLE INFO

Article history:
Received May 17, 2022
Received in revised form July 18, 2022
Accepted December 28, 2022

KEYWORDS:
3cl^{Pro},
andrographolide 2,
covid 19,
in-silico,
pl^{Pro},
rdrp

ABSTRACT

The outbreak of the COVID-19 pandemic in the world has urged researchers to develop a vaccine or therapeutic drugs to fight this virus. This study aimed to assay 14 deoxy-11,12-didehydroandrographolide (AGP 2) ability as an inhibitor of 3-chymotrypsin like-protease (3CL^{Pro}), Papain-like protease (PL^{Pro}), and RNA-dependent RNA-polymerase (RdRp), the viral proteins of SARS-CoV-2 and to evaluate it safeness as a drug candidate. *In-silico* technique was performed in this study to analyze the binding interaction, complex stability between protein and ligand, and drug-likeness properties. The proteins and ligands were obtained from Protein Data Bank (PDB) and PubChem web tools, then using PyRx to identify the binding affinity score, PyMoL to visualize the 3D binding interaction, and WebGro web tools to analyze the stability of each complex. A drug-likeness evaluation was done using SwissADME, pkCSM, and Way2drug web tools. The result of this study showed that the binding affinity score for each complex is; AGP 2-3CL^{Pro} (-6.7 kcal/mol), AGP 2- PL^{Pro} (-6.4 kcal/mol), and AGP 2-RdRp (-7.0 kcal/mol) where the AGP 2-RdRp and AGP 2-3CL^{Pro} showed a stable form indicating the inhibitor ability of AGP 2. This study also demonstrates that the drug-likeness properties of AGP 2 are safe to use. Additionally, it has been proved that AGP 2 can be developed into a therapeutic drug with further studies.

1. Introduction

SARS-CoV-2 is a positive single-strand RNA virus that damages the respiratory tract of mammals, including humans and bats. Like other RNA viruses, SARS-CoV-2 is prone to genetic evolution with the development of mutations while adapting to its new human host. The adaptable ability of this virus was the main reason for its high virality rate. Right after the virus is attached to the human Angiotensin Converting Enzymes (ACE) receptor, it releases the RNA into the human cells. It hijacks the cells' transcription and translation process generating structural and non-structural proteins such as 3CL^{Pro}, PL^{Pro}, and RdRp. These three non-structural proteins play a role in virus pathology function by initiating proteolytic maturation and the formation of the virus Replication-Transcription Complex (RTC). With these functions, SARS-CoV-2 can easily infect the host cells faster and cause casualties in large numbers. According to (Murugan *et al.* 2021), it effectively fights SARS-CoV-2 by inhibiting these viral proteins. Until now, research on using nature drugs as an alternative to tackling this virus using *in silico* techniques is still scarce.

One study was reported in Indonesia and India about *in silico* using plant secondary metabolites fighting 3CL^{Pro}, PL^{Pro}, and RdRp. Fajrin *et al.* (2022.) found that quercetin can inhibit 3CL^{Pro} and PL^{Pro} reviewed on its favorable binding affinity and RMSD value. On the other hand, Pandeya *et al.* (2020) assert that three compounds from *Argemone mexicana*: protopine, allocryptopine, and

* Corresponding Author
E-mail Address: lud@umm.ac.id

6-acetonyldihydrochelerythrine can inhibit RdRp from SARS-CoV-2 effectively.

Plant secondary metabolites believed can be an effective option to propose as the alternative, as most of them are safer and more cost-effective that contain the natural antiviral compound (Koparde *et al.* 2019). Meanwhile, *Andrographis paniculata*, also known as Sambiloto, has been listed by the FDA as one of the medicinal herbs and was widely used for various diseases (Royani *et al.* 2014). In Indonesia, Sambiloto was used to treat various diseases, such as flu and fever, and to decrease blood glucose in diabetic patients (Bahi *et al.* 2020).

Andrographis paniculata was reported to contain a major compound of diterpenoids with various derivatives like andrographolide, 14 deoxy-11, 12-didehydroandrographolide (AGP 2), neoandrographolide, 14-deoxyandrographolide, 14-deoxy-14,15-didehydroandrographolide, andrographanin, and isoandrographolide (Yunita 2021). AGP 2 was believed to exert no toxicity and has higher oral bioavailability than andrographolide. Not just that, it also has many pharmacology activities such as anti-virus. An *in vitro* research from China found that AGP 2 strongly inhibited H5NI replication, and the partial mechanism underlying this effect has been elucidated. This research shows AGP 2 has low cytotoxicity and significantly decreased the protein level of non-structural proteins of the H5N1 virus (Cai *et al.* 2015).

However, whether AGP 2 from *Andrographis paniculata* can exhibit the same result as the previous *in silico* study to fight $3CL^{Pro}$, PL^{Pro}, and RdRp of SARS-CoV-2 still needs to be determined. Due to AGP 2's numerous bioactivities, it should be considered to invent therapeutics that can inhibit and interfere with the viral replication process of the Covid 19 virus. Thus, this study aims to assay AGP 2 ability to possess as an inhibitor to 3-chymotrypsin like-protease ($3CL^{Pro}$), Papain-like protease (PL^{Pro}), and RNA-dependent RNA-polymerase (RdRp), the viral proteins of the virus and to evaluate the pharmacoproperties of 14-deoxy 11, 12-didehydroandrographolide (AGP 2) as a drug candidate using the *in-silico* technique.

2. Materials and Methods

2.1. Docking of Andrographolide 2 to SARS-CoV-2 Proteins

2.1.1. Ligand and Receptors Preparation

The 3D structure of SARS-CoV-2 non-structural proteins (nsp), which is a 3-Chymotrypsin-like protease ($3CL^{Pro}$), Papain-like protease (PL^{Pro}), and RNA-dependent RNA-polymerase (RdRp) were obtained from Protein Data Bank (PDB) with PDB ID of each are $3CL^{Pro}$ (6LU7), PL^{Pro} (7LFU) and RdRp (6NUS). The 14-deoxy 11, 12-didehydroandrographolide's (AGP 2) 3D structure was obtained from PubChem with ID (CID: 5318517) (Lim *et al.* 2021). In this step, the protein must undergo the purification process to eliminate the unwanted segments of the inhibitor before entering the molecular docking step. The purification process was performed using PyMol.

2.1.2. Molecular Docking

Protein-ligand binding docking analysis was performed using PyRx, and the 3D visualization of the interaction was using PyMol. PyRx application tools provide data about the active binding site of the protein receptor with a binding affinity score (Nuryady *et al.* 2021). This study has three binding protein-ligand complexes: AGP 2–$3CL^{Pro}$, AGP 2–PL^{Pro}, and AGP 2–RdRp. The visualized data using PyMol will show the amino acid residues that interacted with the ligand in precise length.

2.1.3. Molecular Dynamic Simulation

All the complexes of the protein-ligand result in this study have been used to perform the molecular dynamics (MD) simulations using the WebGro web tools (https://simlab.uams.edu/). The MD simulations were carried out to study the stability of the complexes formed in the ambient condition based on the RMSD and RMSF values (Murugan *et al.* 2021). The equilibration and MD run parameters were set to default in this web tool as the temperature was set to 300 K, pressure bar 1.0, and the time was set to 20 nanoseconds while the approximate number of frames was 1,000.

2.2. Drug-Likeness Prediction

2.2.1. ADME Prediction Analysis

ADME (Absorption, Distribution, Metabolism, and Excretion) of the drug's pharmacodynamics materials is imperative to analyze. This prediction aims to analyze the drug-likeness of the proposed ligand and whether it is safe to consume by human or animal models. The analysis was done using SwissADME web tools (https://www.swissadme.ch). The data obtained contains information on ligand drug-likeness, such as physicochemical properties, lipophilicity, water-solubility, pharmacokinetics, drug-likeness, and medicinal chemistry (Enmozhi *et al.* 2020a).

The percentage of oral absorption (%ABS) were calculated using the equation from (Zhao *et al.* 2002):

$$\%ABS = 109 - (0.345 \times TPSA)$$

2.2.2. Toxicity Prediction Analysis

Toxicity prediction is essential to predict the drug candidate's tolerability before being ingested into the human and animal models. pkCSM (http://biosig.unimelb.edu.au/pkcsm/prediction) is an online database used in this toxicity prediction. The web tools provide details of ligand's toxicology effects on AMES toxicity, human maximum tolerance dose (HMTD), hERG-I inhibitor, hERG-II inhibitor, LD_{50}, and hepatoxicity (Enmozhi *et al.* 2020b).

2.2.3. Quantitative Structure-Activity Relationship (QSAR) Analysis

The QSAR analysis was then performed to check the feasibility of the ligand's bioactivity using Way2drug web tools (http://way2drug.com/passonline). The ligand's canonical smiles were inserted into the website's command box and examined. The result was shown in the list with the expectation that the ligand possesses antiviral activities against a positive single-stranded RNA virus with indications of passing the threshold of Pa > 0.3.

3. Results

3.1. Molecular Docking

Molecular docking analysis and visualization were done using PyRx and PyMoL databases. Based on Figure 1, the three protein-ligand binding complexes' results are as follows, the AGP 2-RdRp (-7.0 kcal/mol) complex comes with the highest binding affinity score, followed by AGP 2-3CLPro (-6.7 kcal/mol), then AGP 2-PLPro (-6.4 kcal/mol).

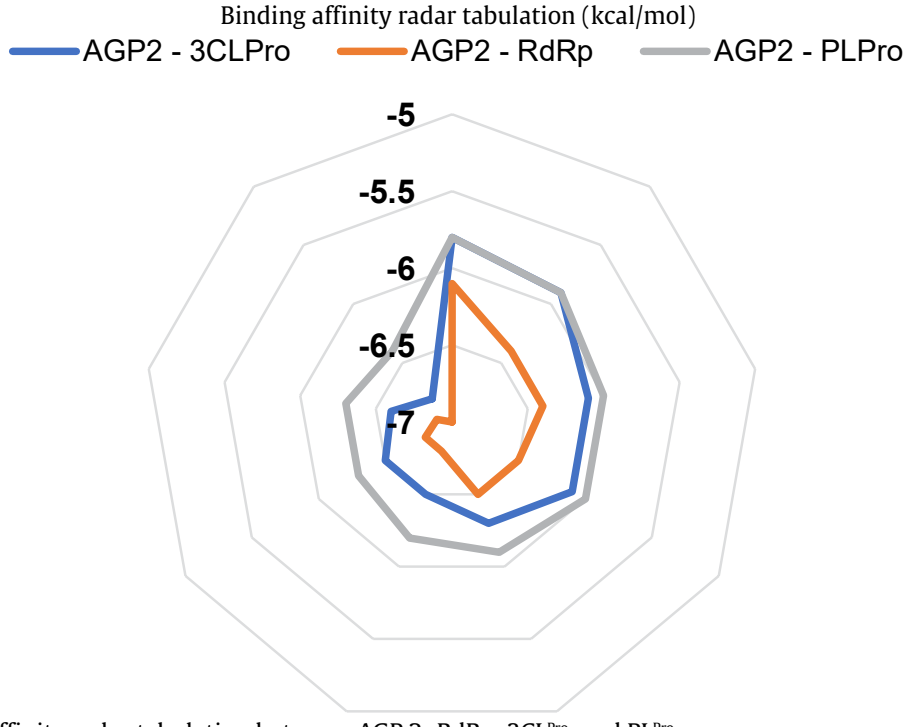

Figure 1. Binding affinity radar tabulation between AGP 2–RdRp, $3CL^{Pro}$, and PL^{Pro}

Figures 2, 3, and 4 show this study's visualization of each complex. Each figure shows the binding interaction between AGP 2 and the proteins where the pink structure is the ligand, and the blue stick is the residues. The yellow line represents the binding interaction with bond-length information.

3.2. Molecular Dynamic Simulation

Figure 5 shows the Molecular Dynamic simulation results. The data on complex stability was reviewed from the Root Mean Square Deviation (RMSD) and Root Mean Square Fluctuation (RMSF). Meanwhile, Table 1 shows the detailed data of the molecular

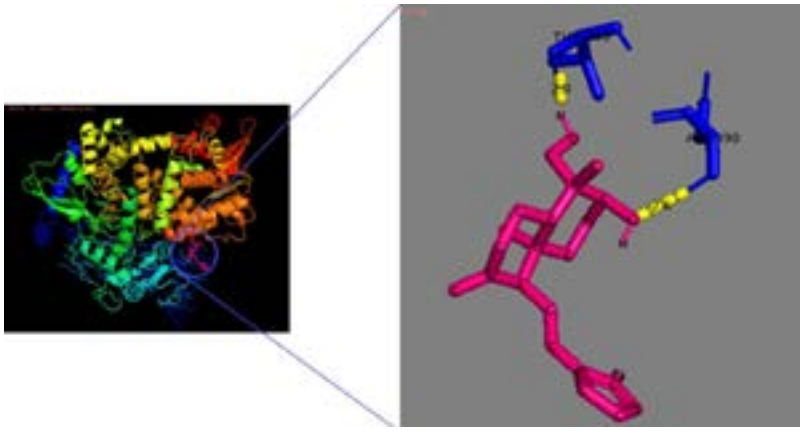

Figure 2. AGP 2–RdRp binding interaction between protein's residues and the ligand

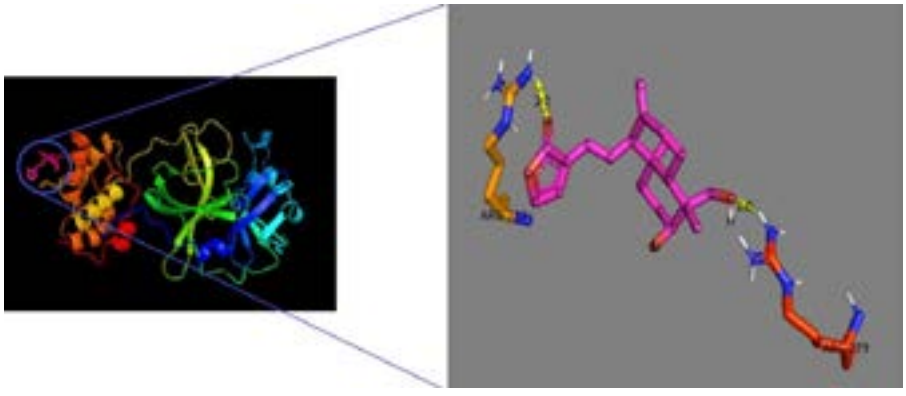

(A)

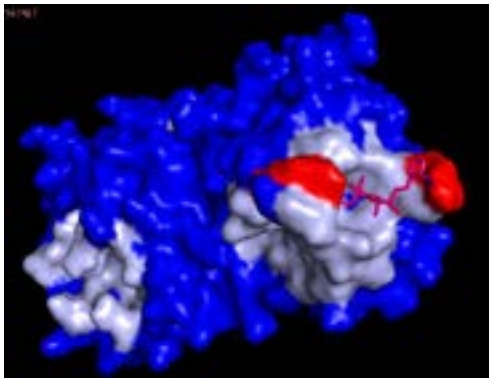

(B)

Figure 3. (A) AGP 2–3CL^{Pro} binding interaction between protein's residues and the ligand, (B) AGP 2–3CL^{Pro} binding interaction in 3D surface visualization. The red area represents the polar binding interaction; meanwhile, the light blue area is the non-polar binding interaction, and the blue area represents the protein structure

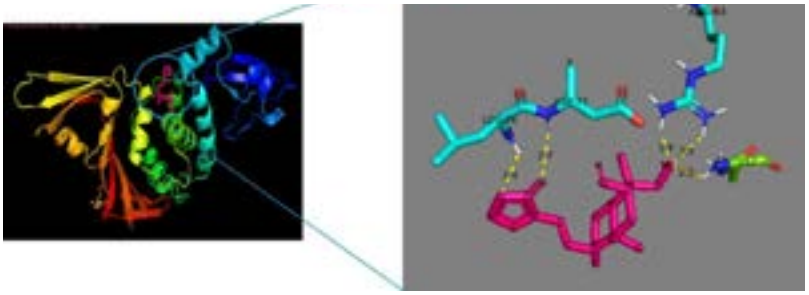

Figure 4. AGP 2–PL^{Pro} binding interaction between protein's residues and the ligand

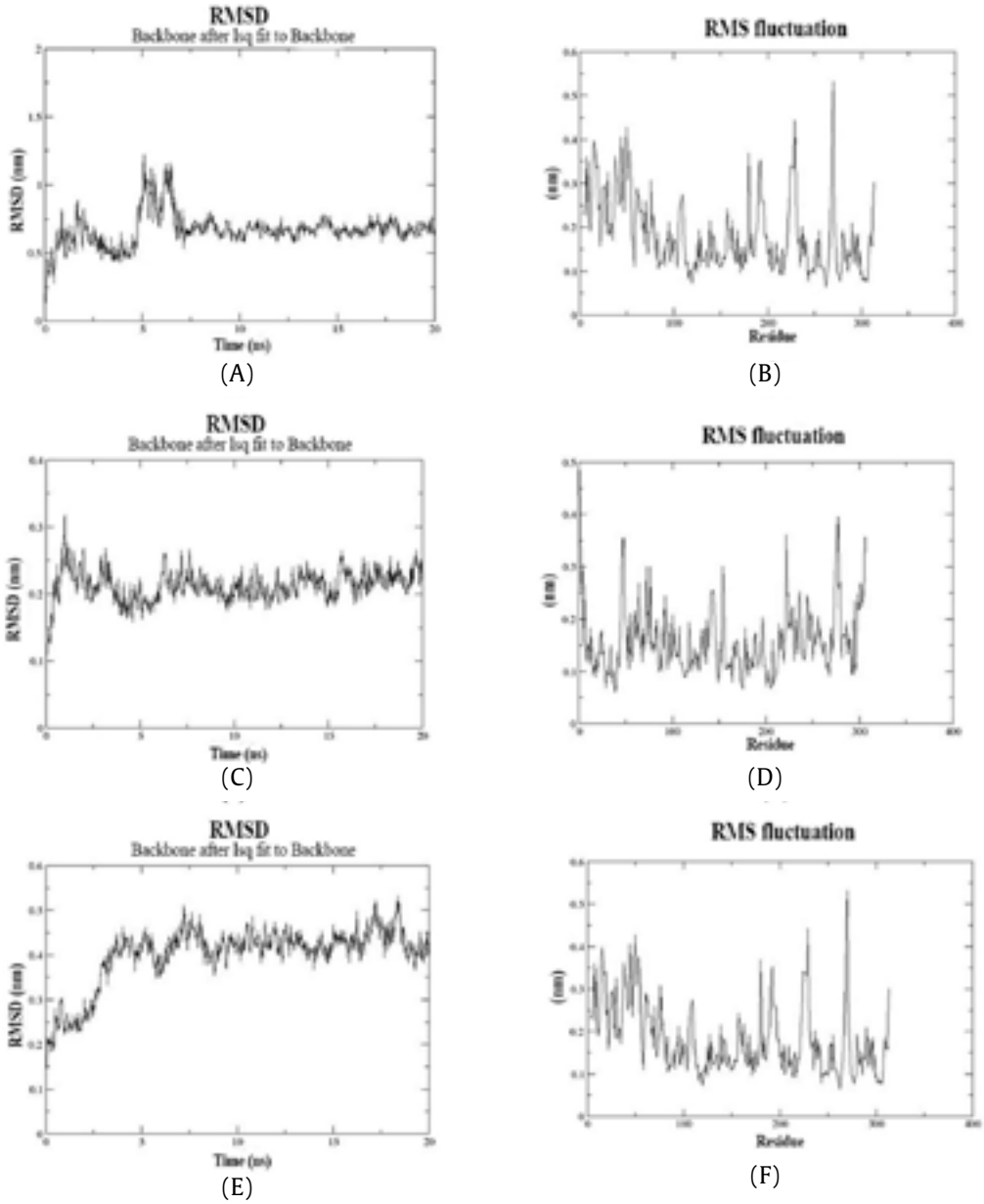

Figure 5. RMSD and RMSF analysis graph: (A) AGP 2–RdRp RMSD, (B) AGP 2–RdRp RMSF, (C) AGP 2–3CL^{Pro} RMSD, (D) AGP 2–3CL^{Pro} RMSF, (E) AGP 2–PL^{Pro} RMSD, (F) AGP 2–PL^{Pro} RMSF

dynamic simulation that shows the AGP 2–PL^{Pro} RMSD value did not obey the threshold, as it is above the standard value. The other two complexes obey the standard threshold of RMSD and RMSF itself.

3.3. ADME Prediction Analysis

Drug candidate screening was done using the Swiss ADME database (Table 2). Based on Lipinski's Rule of Five, there are no violations detected for this drug candidate, as all the parameters showed favorable results.

Figure 6 shows AGP 2 analysis using the Boiled-Egg model. The egg-shaped plot is divided into three parts, including a yolk (BBB access), the white egg (HIA access), and the grey region (no HIA or BBB access). AGP 2 was plotted in the white egg region with the blue color of the dot, indicating that this drug candidate is suitable for oral consumption and acts as the positive substrate of P-glycoprotein (PGP+) in a cellular mechanism.

The bioavailability radar (Figure 7) showed a hexagonal structure, with each vertices representing

Table 1. RMSD and RMSF results

Complexes	Result		Threshold	
	RMSD (Å)	RMSF (Å)	RMSD (Å)	RMSF (Å)
AGP 2–RdRp	0.75	1.4		
AGP 2–3CL^{Pro}	2.2	1.3	3.0	2.5
AGP 2-PL^{Pro}	4.3	1.0, 1.3, 1.4, 1.8		

Table 2. ADME prediction result

Complexes	Pharmacoproperties	Result	Threshold (Yasin *et al.* 2020)
AGP 2	Molecular weight (g/mol)	350.45	500
	Lipophilicity (cLogP)	2.30	<5
	Water solubility (cLogS)	Soluble	Soluble
	Topological polar surface area (TPSA) (Å2)	86.99	40-120
	Number of rotatable bond	3.00	<10
	Hydrogen-bond acceptor	5.00	<10
	Hydrogen-bond donor	3.00	<5
	Oral absorbtion (%ABS)	78.99	Higher is good

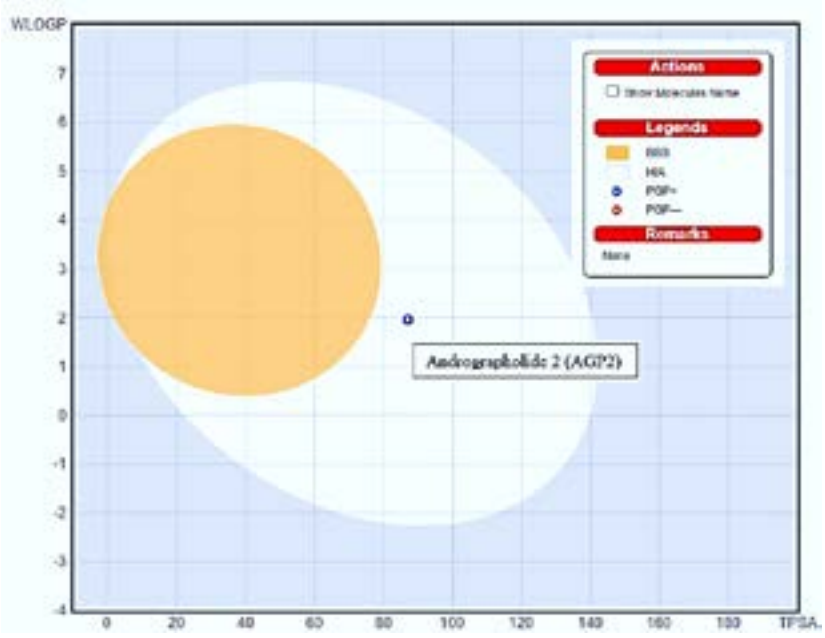

Figure 6. Boiled-egg model

a parameter that defines a bioavailable drug. The pink area within the radar indicates the optimal range for each property (Lipophilicity: XLOGP3 between -0.7 and 5.0, size: MW between 150–500 g/mol, polarity: TPSA between 20–130 Å2, Solubility: Log S (ESOL) not higher than 6, Saturation: fraction of carbons in the sp3 hybridization not less than 0.25 and Flexibility: not more than nine rotatable bonds).

Table 3 shows the bioavailability result of AGP 2. All these results showed that each parameter was in the optimal range. Bioavailability is the extent and rate to which the active drug ingredient or active moiety from the drug product is absorbed and becomes available at a site of drug action.

3.4. Toxicity Prediction Analysis

The toxicity prediction of the drug candidate was made using pkCSM web tools. This screening of toxicity for the drug includes AMES toxicity, human maximum tolerated dose (HMTD), hERG I and hERG II inhibition, LD_{50}, and hepatoxicity analysis (Table 4). The results showed no violation in this screening, indicating that the toxicity of AGP 2 is good.

3.5. QSAR Analysis

The QSAR analysis (Table 5) showed that three related bioactivities are necessary for this research objective's success, including antiviral activities and RNA synthesis inhibitors. The Probable Active

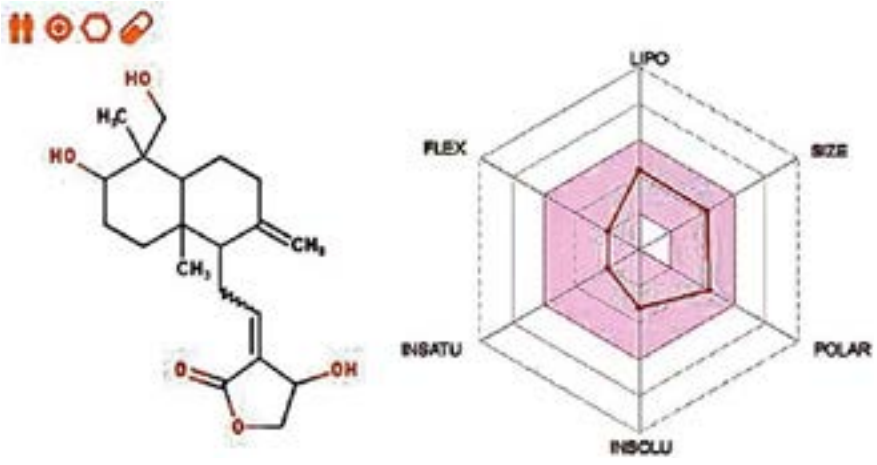

Figure 7. Bioavailability radar of AGP 2

Table 3: Bioavailability radar's result

LIPO	FLEX	INSATU	INSOLU	POLAR (Å2)	SIZE (g/mol)
2.16	3	0.75	-3.18	86.99	350.45

Lipophilicity (LIPO), flexibility (FLEX), insaturation (INSATU), insolubility (INSOLU), and polarity (POLAR)

Table 4: Toxicity prediction results

AMES	HMTD (log mg/kg/day)	hERG I	hERG II	LD_{50} (mg/kg)	Hepatotoxicity
No	0.128	No	No	2,162	No

Mutagenesis (AMES), human maximum tolerated dose (HMTD), and median lethal dose (LD_{50})

Table 5. QSAR analysis result

Bioactivity	Pa Score
Antiviral (Rhinovirus)	0.367
Antiviral (General)	0.424
RNA synthesis inhibitor	0.436

(Pa) score of all the related bioactivities is shown in Table 5. The threshold of the ligand Pa score based on QSAR analysis should be Pa >3.0, indicating the ligand is close to active.

4. Discussion

4.1. Molecular Docking

Figure 1 shows a binding affinity radar tabulation, where each non-structural protein has nine active binding sites as the results of PyRx analysis. The outer number of the nonagon-structure vertices represents the active binding site, with sequence number one hitting the highest binding affinity complex score and number nine being the lowest score. Based on the results, the AGP 2–RdRp complex showed the highest binding affinity with a score of -7.0 kcal/mol, followed by AGP 2–3CL^{Pro} with a score of -6.7 kcal/mol and AGP 2–PL^{Pro} with a score of -6.4 kcal/mol. In this study, all the complexes have a binding affinity range from -6.4 kcal/mol to -7.0 kcal/mol. In comparison with the existing drugs (remdesivir and molnupiravir) with a binding affinity range from -6.6 kcal/mol (Murugan *et al.* 2021) up to -7.5 kcal/mol (Sharov *et al.* 2022) AGP 2 showed an excellent binding affinity since the score range was not significantly different.

AGP 2–3CL^{Pro} binding interaction between protein's residues and the ligand; (b) AGP 2–3CL^{Pro} binding interaction in 3D surface visualization. The red area represents the polar binding interaction; meanwhile, the light blue area is the non-polar binding interaction, and the blue area represents the protein structure.

The active binding site of AGP 2–RdRp was located in the palm domain (Figure 2), aligning with the previous research from (Zhu *et al.* 2020). In this interaction, two hydrogens formed with two residues, namely Thr-393 and Asp-390, where Thr-393 acted as the hydrogen-bond acceptor and Asp-390 as the hydrogen-bond donor. Meanwhile, the AGP 2–3CL^{Pro} complex (Figure 3) shows the formation of two hydrogen bonds and a polar binding with the ligand at the protein's surface. This active binding site is linear with the study from (Mody *et al.* 2021), which claims the active binding site in his study is located at the protein's surface. However, the interacted residues in this study (Arg-222, Arg-279) acted as the hydrogen-bond donor to the ligand. It differs from Liu *et al.* (2020) mentioned that the dyad residues (His-41 and Cys-145) are the main elements forming a hydrogen bond with the ligand.

Moreover, the AGP 2–PLPro complex (Figure 4) showed five hydrogen bonds bonded to four residues, Asp-77, Arg-83, Asn-157 and Leu-76, acting as the hydrogen-bond donor to the ligand. Uniquely, Leu-76 formed a hydrogen bond with the ligand even though this residue is classified as a non-polar element. However, based on (Matthews 2001), leucine (Leu) has a side chain with a polar atom that can interact with other polar molecules, and these abilities are known as amphiphilic.

Based on all the complex results in this step, all their interactions were categorized as strong bonds due to their bond-length interaction being less than 3.0 Å2 (Arba *et al.* 2020). Yan *et al.* (2017) also stated that a hydrogen bond less than 3.0 Å2 exhibits a strong bonding interaction and most likely exhibits a promising inhibitor characteristic.

4.2. Molecular Dynamic Simulation

Based on the Molecular Dynamic Simulation result in Figure 5 and Table 1, these complexes, AGP 2–RdRp and AGP 2-3CL^{Pro}, exert good stability after the binding interaction occurs. The RMSD and RMSF value for both complexes obey the standard threshold of this study. According to (Fuglebakk *et al.* 2012), the RMSD value should be below 3.0 Å. The lower value of RMSD means the conformational changes in the complex are scarce; hence it is a stable binding. As for the RMSF, Fatriansyah *et al.* (2022) stated that if the value is below 2.5 Å, the fluctuation of the residues is low, which means the complex binding is stable. Since both complexes showed a value below all the criteria of RMSD and RMSF, the complexes manifest a strong and stable interaction. As for the AGP 2–PL^{Pro} complex, the RMSD result showed a high value above the standard threshold. Even if the RMSF value of this complex is below the threshold, this complex is classified as not stable binding because the conformational change of this complex is high.

4.3. ADME Prediction Analysis

Based on the ADME prediction analysis results (Table 2), all the pharmacoproperties of AGP 2 showed a good result, as all the criteria of Lipinski's Rule of Five were obeyed. From the Boiled-egg model evaluation (Figure 6), AGP 2 was indicated to

be suitable for oral consumption through intestinal absorption (Suhud *et al.* 2019).

The molar refractivity and %ABS score of AGP 2 showed a significant number of 95.21 and 78.99%, which indicates that AGP 2 has good membrane permeability (Guan *et al.* 2019). The favorable condition justifies that AGP 2 is permeable through particular membranes and can remain constant even amid strong or weak solvent-solvent or solute-solvent interactions (Enmozhi *et al.* 2020b). (Tong *et al.* 2019) stated that high bioavailability is associated with a lower molecular weight and TPSA. Linearly with AGP 2 physicochemical properties in this study (Figure 7 and Table 3).

The pharmacokinetics data predicted no violation of metabolism for CYP1A2, CYP2C19, CYP2D9, CYP2D6, and CYP3A4. These Main cytochromes (CYP) refer to various metabolism and interaction inside the human body (Durán-Iturbide *et al.* 2020) AGP 2 does not stop liver metabolism by inhibiting CYP1A2 (Sugiono *et al.* 2018); it also does not interfere with the metabolism of several therapeutic drugs, especially anti-convulsants, anti-ulcer, anti-malarial, anesthetic, and sedative drugs by inhibiting CYP2C19 (Lee *et al.* 2018). As for the metabolism of β blockers, anti-hypersensitive drugs, anti-arrhythmic drugs, and anti-depressants will not stop by AGP 2 as it does not inhibit CYP2D6 (Taylor *et al.* 2020). AGP 2 also does not inhibit CYP2C9 which results in the metabolism of anti-clotting agents, anti-hypersensitive, anti-hypertensive, management of Type II Diabetes and Nonsteroidal Anti-Inflammatory (NSAIDs) (Park *et al.* 2021). The CYP3A4 was not inhibited by AGP 2, which caused the oxidation of fatty acids, steroids, xenobiotics, and hormone synthesis (Samuels and Sevrioukova 2021).

4.4. Toxicity Prediction Analysis

AMES toxicity prediction (Table 4) showed that no mutagenesis/DNA damage could happen because of the AGP 2 intake. AGP 2 is classified as a non-genotoxic carcinogen that can act through DNA-damaging mechanisms (Arriaga-alba *et al.* 2012). This prediction also provides a human maximum tolerated dose (HMTD); it is predicted that HMTD was 0.128 log mg/kg/day. This dose aimed to maximize the benefit of the drug and minimize the harm. It should be known that the HMTD varies between patients' acute, maintenance, and preventive therapy. The proper dose secures the effective maintenance treatment, minimization of adverse side effects, tolerability, and long-term adherence to the drug intake (Stampfer *et al.* 2019). The ion-gated channels hERG I and hERG II were predicted to be secure from AGP 2 inhibition; thus, they can perform their task safely. LD_{50} value in this study was 2.162 mg/kg, which indicates AGP 2 is classified in class IV of toxicity (500–5,000 mg/kg). The highest the value of LD_{50}, the more tolerance to poisoning it is (Worasuttayangkurn *et al.* 2019). The AGP 2 was predicted to not cause oxidative stress in the liver due to DNA damage, lipid peroxidation, and protein dysfunction (Fikry and Ahmed 2019). In overall toxicity analysis, AGP 2 was predicted not to cause and lead to health issues and was safe to consume.

4.5. QSAR Analysis

Renatha *et al.* (2022) stated that the threshold of the ligand Pa score based on QSAR analysis should be Pa >3.0. Based on the result from the QSAR analysis in Table 5, AGP 2 is expected to have many bioactivities. In this study, the ligand should be predicted to possess the ability as an antiviral against a positive single-strand RNA virus. As the target proteins used in this study play an important role in the SARS-CoV-2 replication process, thus the proposed ligand must fight the RNA synthesis mechanism of the virus. From a previous *in-silico* study, the diterpenoids and their derivatives (andrographolide, 14 deoxy-11, 12-didehydroandrographolide (AGP 2), neoandrographolide, 14-deoxyandrographolide) effectively inhibited the spike protein from SARS-CoV-2 with considerable binding affinity from the range -6.7 kcal/mol to -7.8 kcal/mol (Murugan *et al.* 2021). As the proposed ligand's bioactivity exceeds the threshold, it can be against the non-structural proteins of SARS-CoV-2, including $3CL^{Pro}$, PL^{Pro}, and RdRp.

In conclusion, based on our findings, AGP 2 possesses the capability as a suitable inhibitor candidate in fighting RdRp, $3CL^{Pro}$, and PL^{Pro} from SARS-CoV-2 as its binding affinity score were -7.0 kcal/mol, -6.7 kcal/mol, and -6.4 kcal/mol respectively. The molecular dynamic simulation analysis then uncovers that the AGP 2-RdRP and AGP 2-$3CL^{Pro}$ complexes are steady, barring AGP 2-PL^{Pro}. As for the drug-likeness analysis and evaluation, it showed that AGP 2 heeds all the benchmarks of

the safety indicator for drugs, including absorption, distribution, metabolism, excretion, and toxicity. Since the binding affinity, stability, and drug-likeness of the formed complexes and AGP 2 compound itself is adequate, it verified that AGP 2 could be materialized as a drug candidate for combating Covid 19 through extensive research in the future.

Acknowledgements

We want to express our sincere thanks to Muhammad Yusril Ihya' Maksum for his help with the device of this research and his support with all the small things in this research-making process that came out as a big help for this success. The authors acknowledge the facilities and technical support of the University of Muhammadiyah Malang library, where the research report was done.

References

Arba, M., Nur-hidayat, A., Usman, I., Yanuar, A., Wahyudi, S.T., Fleischer, G., Brunt, D.J., Wu, C., 2020. Virtual screening of the indonesian medicinal plant and zinc databases for potential inhibitors of the RNA-dependent RNA polymerase (RdRp) of 2019 novel coronavirus. *Indonesia Journal Chemistry*. 20, 1430–1440. https://doi.org/10.22146/ijc.56120

Arriaga-alba, M., Montoya, R.M., Aguirre, J.J.E., 2012. The ames test in twenty-first century the ames test in twenty-first century. *A Journal of Toxicology*. 2, 23–37.

Bahi, R.R.R., Herowati, R., Harmastuti, N., 2020. Studi biokemoinformatika kandungan kimia daun sambiloto (*Andrographis paniculata* (Burm. f.) Nees) sebagai antihiperglikemia serta prediksi parameter farmakokinetik dan toksisitas. *Jurnal Farmasi Indonesia*. 17, 466–477.

Cai, W., Li, Y., Chen, S., Wang, M., Zhang, A., Zhou, H., Chen, H., Jin, M., 2015. 14-Deoxy-11,12-dehydroandrographolide exerts anti-influenza A virus activity and inhibits replication of H5N1 virus by restraining nuclear export of viral ribonucleoprotein complexes. *Antiviral Research*. 118, 82–92. https://doi.org/10.1016/j.antiviral.2015.03.008

Durán-Iturbide, N.A., Díaz-Eufracio, B.I., Medina-Franco, J.L., 2020. *In silico* ADME/tox profiling of natural products: a focus on BIOFACQUIM. *ACS Omega*. 5, 16076–16084. https://doi.org/10.1021/acsomega.0c01581

Enmozhi, S.K., Raja, K., Sebastine, I., Joseph, J., 2020a. Andrographolide as a potential inhibitor of SARS-CoV-2 main protease: an *in silico* approach. *Journal of Biomolecular Structure and Dynamics*. 39 , 3092–3098. https://doi.org/10.1080/07391102.2020.1760136

Enmozhi, S.K., Raja, K., Sebastine, I., Joseph, J., 2020b. Andrographolide as a potential inhibitor of SARS-CoV-2 main protease: an *in silico* approach. *Journal of Biomolecular Structure and Dynamics*. 39 , 3092–3098. https://doi.org/10.1080/07391102.2020.1760136

Fajrin, I., Aryanti, K., Susilo, J., 2022. The sar-cov2 inhibitor of quercetin activity. A docking molecular studies on 3CLpro, PLpro, and NSP3. *Indonesian Journal of Pharmacy and Natural Product*. 5, 97–107. https://doi.org/https://doi.org/10.35473/ijpnp.v5i2.1789

Fatriansyah, J.F., Rizqillah, R.K., Yandi, M.Y., Fadilah, Sahlan, M., 2022. Molecular docking and dynamics studies on propolis sulabiroin-A as a potential inhibitor of SARS-CoV-2. *Journal of King Saud University - Science*. 34, 101707. https://doi.org/10.1016/j.jksus.2021.101707

Fikry, E.M., Ahmed, A.Y., 2019. Hepatotoxicity and antioxidants: an overview. *Journal of Drug Delivery and Therapeutics*. 9, 1068–1077. https://doi.org/http://dx.doi.org/10.22270/jddt.v9i3-s.3089

Fuglebakk, E., Echave, J., Reuter, N., 2012. Measuring and comparing structural fluctuation patterns in large protein datasets. *Bioinformatics*. 28, 2431–2440. https://doi.org/10.1093/bioinformatics/bts445

Guan, L., Yang, H., Cai, Y., Sun, L., Di, P., Li, W., Liu, G., Tang, Y., 2019. ADMET-score-a comprehensive scoring function for evaluation of chemical drug-likeness. *Med. Chem. Comm*. 10, 148–157. https://doi.org/10.1039/C8MD00472B

Koparde, A.A., Doijad, R.C., Magdum, C.S., 2019. Natural Products in drug discovery. *Pharmacognosy-Medicinal Plants*. ... , ...-... .

Lee, C.R., Sriramoju, V.B., Cervantes, A., Howell, L.A., Varunok, N., Madan, S., Hamrick, K., Polasek, M.J., Lee, J.A., Clarke, M., Cicci, J.D., Weck, K.E., Stouffer, G.A., 2018. Clinical outcomes and sustainability of using CYP2C19 genotype-guided antiplatelet therapy after percutaneous coronary intervention. *Circulation. Genomic and Precision Medicine*. 11, 1–12. https://doi.org/10.1161/CIRCGEN.117.002069

Lim, X.Y., Chan, J.S.W., Tan, T.Y.C., Teh, B.P., Mohd Abd Razak, M.R., Mohamad, S., Syed Mohamed, A.F., 2021. *Andrographis paniculata* (Burm. F.) wall. ex nees, andrographolide, and andrographolide analogues as SARS-CoV-2 antivirals? a rapid review. *Natural Product Communications*. 16, 1–15. https://doi.org/10.1177/1934578X211016610

Liu, Y., Liang, C., Xin, L., Ren, X., Tian, L., Ju, X., Li, H., Wang, Y., Zhao, Q., Liu, H., Cao, W., Xie, X., Zhang, D., Wang, Y., Jian, Y., 2020. The development of Coronavirus 3C-Like protease (3CLpro) inhibitors from 2010 to 2020. *European Journal of Medicinal Chemistry*. 206, 1–19. https://doi.org/10.1016/j.ejmech.2020.112711

Matthews, B.W., 2001. Hydrophobic interactions in proteins. *In Encyclopedia of Life Sciences*. pp. 1–6. https://doi.org/10.1038/npg.els.0002975

Mody, V., Ho, J., Wills, S., Mawri, A., Lawson, L., Ebert, M.C.C.J.C., Fortin, G.M., Rayalam, S., Taval, S., 2021. Identification of 3-chymotrypsin like protease (3CL^{Pro}) inhibitors as potential anti-SARS-CoV-2 agents. *Communications Biology*. 4, 1–10. https://doi.org/10.1038/s42003-020-01577-x

Murugan, N.A., Pandian, C.J., Jeyakanthan, J., 2021. Computational investigation on *Andrographis paniculata* phytochemicals to evaluate their potency against SARS-CoV-2 in comparison to known antiviral compounds in drug trials. *Journal of Biomolecular Structure and Dynamics*. 39, 4415–4426. https://doi.org/10.1080/07391102.2020.1777901

Nuryady, M.M., Nurcahyo, R.W., Hindun, I., Fatmawati, D., 2021. Multidrug resistance protein structure of *Trypanosoma evansi* isolated from buffaloes in Ngawi District, Indonesia: a bioinformatics analysis. *Veterinary World*. 14, 33–39. https://doi.org/10.14202/VETWORLD.2021.33-39

Pandeya, K.B., Ganeshpurkar, A., Mishra, M.K., 2020. Natural RNA dependent RNA polymerase inhibitors: molecular docking studies of some biologically active alkaloids of *Argemone mexicana*. *Medical Hypotheses*. 144, 1-6. https://doi.org/10.1016/j.mehy.2020.109905

Park, Y.A., Song, Y., Bin, Yee, J., Yoon, H.Y., Gwak, H.S., 2021. Influence of cyp2c9 genetic polymorphisms on the pharmacokinetics of losartan and its active metabolite e-3174: a systematic review and meta-analysis. *Journal of Personalized Medicine*. 11, 1–9. https://doi.org/10.3390/jpm11070617

Renatha, R.R., Liga, A.R., Bianca, T.C., Denovian, L.X., Budiyanto, S.L., Parikesit, A.A., 2022. Flavonoids as potential inhibitors of dengue virus 2 (DENV2) envelope protein. *Journal of Pharmacy and Pharmacognosy Research* 10, 660–675. https://doi.org/10.5281/zenodo.6558704

Royani, J.I., Hardianto, D., Wahyuni, S., 2014. Analysis of andrographolide contents on sambiloto plants (*Andrographis paniculata*) derived from 12 locations in Java Island. *Bioteknologi & Biosains Indonesia*, 1, 15–20.

Samuels, E.R., Sevrioukova, I.F., 2021. Rational design of CYP3A4 inhibitors: a one-atom linker elongation in ritonavir-like compounds leads to a marked improvement in the binding strength. *International Journal of Molecular Sciences*. 22, 1–22. https://doi.org/10.3390/ijms22020852

Sharov, A.V., Burkhanova, T.M., Tok, T.T., Babashkina, M.G., Safin, D.A., 2022. Computational analysis of molnupiravir. *International Journal of Molecular Sciences*. 23, 1-18. https://doi.org/10.3390/ijms23031508

Stampfer, H.G., Gabb, G.M., Dimmitt, S.B., 2019. Why maximum tolerated dose? *British Journal of Clinical Pharmacology*. 85, 2213–2217. https://doi.org/10.1111/bcp.14032

Sugiono, E., Wijaya, A., Santoso, A., Sandra, F., Patellongi, I.J., Yusuf, I., 2018. Frequencies of CYP1A2 single nucleotide polymorphism in Indonesian and its effect on blood pressure. *Indonesian Biomedical Journal* 10, 297–302. https://doi.org/10.18585/inabj.v10i3.374

Suhud, F., Tjahjono, D.H., Yuniarta, T.A., Putra, G.S., Setiawan, J., 2019. Molecular docking, drug-likeness, and ADMET study of 1-benzyl-3-benzoylurea and its analogs against VEGFR-2. *IOP Conference Series: Earth and Environmental Science*. 293, 1–9. https://doi.org/10.1088/1755-1315/293/1/012018

Taylor, C., Crosby, I., Yip, V., Maguire, P., Pirmohamed, M., Turner, R.M., 2020. A review of the important role of cyp2d6 in pharmacogenomics. *Genes*. 11, 1–22. https://doi.org/10.3390/genes11111295

Tong, Y., Zhang, Q., Shi, W., Wang, J., 2019. Mechanisms of oral absorption improvement for insoluble drugs by the combination of phospholipid complex and SNEDDS. *Drug Delivery*. 26, 1155–1166. https://doi.org/10.1080/10717544.2019.1686086

Worasuttayangkurn, L., Nakareangrit, W., Kwangjai, J., Sritangos, P., Pholphana, N., Watcharasit, P., Rangkadilok, N., Thiantanawat, A., Satayavivad, J., 2019. Acute oral toxicity evaluation of *Andrographis paniculata*-standardized first true leaf ethanolic extract. *Toxicology Reports*. 6, 426–430. https://doi.org/10.1016/j.toxrep.2019.05.003

Yan, Y., Wang, W., Sun, Z., Zhang, J.Z.H., Ji, C., 2017. Protein-ligand empirical interaction components for virtual screening. *Journal of Chemical Information And Modelling*. 5, 1-40. https://doi.org/10.1021/acs.jcim.7b00017

Yasin, S.A., Azzahra, A., Ramadhan, N.E., Mylanda, V., 2020. Studi penambatan molekuler dan prediksi ADMET senyawa bioaktif beberapa jamu Indonesia terhadap SARS-CoV-2 main protease (Mpro). *Berkala Ilmiah Mahasiswa Farmasi Indonesia*. 7, 24–41. https://doi.org/10.48177/bimfi.v7i2.45

Yunita, E., 2021. Mekanisme kerja andrografolida dari sambiloto sebagai senyawa antioksidan. *Herb-Medicine Journal*. 4, 43. https://doi.org/10.30595/hmj.v4i1.8825

Zhao, Y.H., Abraham, M.H., Le, J., Hersey, A., Luscombe, C.N., Beck, G., Sherborne, B., Cooper, I., 2002. Rate-limited steps of human oral absorption and QSAR studies. *Pharmaceutical Research*. 19, 1446–1457. https://doi.org/10.1023/A:1020444330011

Zhu, W., Chen, C.Z., Gorshkov, K., Xu, M., Lo, D.C., Zheng, W., 2020. RNA-dependent RNA polymerase as a target for COVID-19 drug discovery. *SLAS Discovery*. 25, 1141–1151. https://doi.org/10.1177/2472555220942123